

A&A manuscript no.
(will be inserted by hand later)

Your thesaurus codes are:
06 (08.09.2 08.05.2 13.18.5 13.25.5)

ASTRONOMY
AND
ASTROPHYSICS

October 2, 2018

Evidence of $H\alpha$ periodicities in LS I+61°303

R.K. Zamanov¹, J. Martí², J.M. Paredes³, J. Fabregat⁴, M. Ribó³, and A.E. Tarasov⁵

¹ National Astronomical Observatory Rozhen, P.O.Box 136, BG-4700 Smoljan, Bulgaria

² Departamento de Física, Escuela Politécnica Superior, Universidad de Jaén, C/ Virgen de la Cabeza, 2, E-23071 Jaén, Spain

³ Departament d'Astronomia i Meteorologia, Universitat de Barcelona, Av. Diagonal 647, E-08028 Barcelona, Spain

⁴ Departamento de Astronomía, Universidad de Valencia, E-46100 Burjassot, Valencia, Spain

⁵ Crimean Astrophysical Observatory, 334413 Nauchny, Crimea, Ukraine

Received / Accepted

Abstract. We present the results of analyzing $H\alpha$ spectra of the radio emitting X-ray binary LS I+61°303. For the first time, the same 26.5 d radio period is clearly detected in the $H\alpha$ emission line. Moreover, the equivalent width and the peak separation of the $H\alpha$ emission line seem also to vary over a time scale of 1600 days. This points towards the ~ 4 yr modulation, detected in the radio outburst amplitude, being probably a result of variations in the mass loss rate of the Be star and/or density variability in the circumstellar disk. In addition, the dependence of the peak separation from the equivalent width informs us that the LS I+61°303 circumstellar disk is among the densest of Be-stars.

Key words: stars: individual: LS I+61°303– stars: emission line, Be – radio continuum: stars – X-ray: stars

1. Introduction

The Be/X-ray binary LS I+61°303 (V615 Cas) is the optical counterpart of the highly variable radio source GT 0236+610, which exhibits radio outbursts every 26.4917 ± 0.0025 d assumed to be the orbital cycle (Taylor & Gregory 1984; Gregory et al. 1999). The radial velocity measurements of Hutchings & Crampton (1981) are consistent with this interpretation and suggest an eccentric orbit ($e \simeq 0.6$). The same 26.5 d period has been detected in the UBVRI photometric observations of Mendelson & Mazeh (1994), in the infrared (Paredes et al. 1994) and in the soft X-ray flux (Paredes et al. 1997). The amplitude of the periodic variations is $\lesssim 0.2$ magnitudes in the optical and infrared, while the X-ray luminosity of the system often evolves within the range 10^{33} to 6×10^{34} erg s⁻¹ (Bignami et al. 1981; Paredes et al. 1997). LS I+61°303 is also currently regarded today as a serious counterpart candidate to the γ -ray source 2CG 135+01 (Gregory & Taylor 1978; Kniffen et al. 1997; Strickman et al. 1998).

The LS I+61°303 radio emission has been interpreted as synchrotron radiation from relativistic particles. The dependence of the radio outburst flux density on frequency, the time

delay in the outburst peak, and the general shape of the radio light curves can be modeled as continuous injection of relativistic particles into an adiabatically expanding plasma cloud or plasmon (Paredes et al. 1991). It has been proposed that the genesis of such plasmons could be the result of the transition of the neutron star companion from the Propeller to the Ejector regime (Zamanov 1995). Alternatively, a young radio pulsar may also be responsible for the radio emission (Maraschi & Treves 1981; Tavani 1994). The ejector regime would then apply over the whole orbital period, with the flaring radio emission resulting from the variable position of the shock front between the Be star wind and the relativistic wind of the pulsar. Supercritical accretion models during the periastron passage (e.g. Taylor et al. 1992) were also widely accepted in the recent past. However, they appear now very difficult to reconcile with the confirmed sub-Eddington X-ray luminosity of LS I+61°303.

On the other hand, a strong modulation in the amplitude of the 26.5 d periodic radio outbursts, on a time scale of ~ 4 yr, was noticed independently by Paredes (1987) and Gregory et al. (1989). This modulation has been recently confirmed after a Bayesian analysis of 20 yr of LS I+61°303 radio data by Gregory (1999). Two possible scenarios have been considered in order to account for such a long-term variability: the precession of relativistic jets or, alternatively, the variable accretion rate due to quasi-cyclic Be-star envelope variations (Gregory et al. 1989).

The optical spectrum of LS I+61°303 corresponds to a rapidly rotating B0V star with a stable equatorial disk and mass loss (Hutchings & Crampton 1981). $H\alpha$ observations of this star have been discussed, among others, by Gregory et al. (1979), Paredes et al. (1994) and Zamanov et al. (1996). In these papers, it was noticed a significant variability of the red and blue humps at opposite locations of the orbit. On the other hand, the quasi simultaneous $H\alpha$ and radio observations by Zamanov et al. (1996) did not indicate considerable changes in $H\alpha$ close to the radio maximum. This fact is in agreement with the assumption that the $H\alpha$ emission comes mainly from the Be star disk, and the radio outbursts are related to the compact object. Another interesting property of the $H\alpha$ emission is

its very broad wings, achieving $FWZI \sim 3000 \text{ km s}^{-1}$. Unfortunately, most LS I+61°303 spectra available do not have sufficient SNR to investigate this intriguing feature.

In this paper, we present 84 new H α observations of LS I+61°303 which are analyzed together with the data from Paredes et al. (1994) and Zamanov et al. (1996). We report the clear detection of a 26.5 d periodicity in some parameters of the H α emission line. In addition, our extended spectroscopic database interestingly suggests the presence of a 1600 d modulation in the H α equivalent width. These new H α periods seem to match closely those known at radio wavelengths. The possible implications of all these findings are pointed out and discussed.

2. Observations

Our H α spectroscopic observations of LS I+61°303 were carried out using different astronomical facilities. The results of this observations are summarized in Table 1.

A total of 60 new spectra were obtained with the Coudé spectrograph of the 2.0 m RCC telescope at the Bulgarian National Astronomical Observatory “Rozhen”, between October 1993 and August 1998. An ISTA-CCD with 400×580 pixel was used as a detector. The spectrum coverage is about 110 \AA , with a dispersion of $0.2 \text{ \AA pixel}^{-1}$. Usually 2 or 3 exposures, of 20 minutes each, were always taken to improve the sensitivity and to avoid problems with eventual cosmic ray hits. The “Rozhen” observations have been processed using the 3A software (Ilyin 1997) and the IRAF package of NOAO (Tucson, Arizona). It deserves noting that the new Rozhen data from Ro931031 to Ro980805 are a uniform data set.

We have also used 17 more spectra obtained within the framework of the Southampton and Valencia Universities collaborative program on high-mass X-ray binaries (Coe et al. 1993; Reig et al. 1997a). 14 of them were obtained with the Richardson-Brearly Spectrograph at the Cassegrain focus of the Jakobus Kaptein Telescope, La Palma, Spain. Different gratings were used, giving dispersions between 0.33 and $1.34 \text{ \AA pixel}^{-1}$. The remaining 3 spectra were obtained with the P-60 Cassegrain Echelle Spectrograph in regular grating mode at $0.8 \text{ \AA pixel}^{-1}$, attached to the 1.5-m telescope of the Palomar Mountain Observatory. These data were reduced using the *Figaro* (Shortridge & Meyerdicks 1996) and *Dipso* (Howarth et al. 1996) packages included in the STARLINK software collection.

Additionally, we also include 7 H α spectra from the 2.6 m telescope at the Crimean Astrophysical Observatory. They were obtained at the Coudé focus of this instrument with a dispersion of $0.066 \text{ \AA pixel}^{-1}$ and a coverage of about 67 \AA . The detector used was a Photometrics SDS-9000 with a EVV 15-11 1024×256 pixel CCD.

In order to ensure a unified post-processing of the spectra, all of them were normalized with respect to the local continuum. When possible the same continuum regions were used at $6520\text{--}6530$ and $6595\text{--}6605 \text{ \AA}$, located at the blue and red side of

the H α emission line, respectively. The underlying continuum was rectified to unity by employing a linear fit.

On each spectrum, we have measured the total equivalent width of the H α emission line (hereafter $EW(\text{H}\alpha)$), the heliocentric radial velocities of the central dip, blue and red humps, the ratio between the equivalent widths of the blue and red humps, the B/R ratio and the $FWHM$ of the humps. The dates of observations and the measured quantities are summarized in Table 1. The $FWHM$ and the radial velocities were measured by employing a Gaussian fit. The $FWHM$ was corrected for the instrumental broadening. The errors depend mostly on the dispersion, and we estimate them to be about 10% for the EW s, about 1/2 pixel for the radial velocities, ± 0.04 in the B/R ratios and 1 pixel for the $FWHM$ s.

Some previously published Rozhen spectra, those from Ro920903 to Ro 930909 in Table 1, have been processed again to be used in this work. We will also include in our analysis the H α parameters listed in the Table 4 of Paredes et al. (1994), whose $EW(R)/EW(B)$ header should be actually the inverse.

3. Results

3.1. A very dense circumstellar disk in LS I+61°303

It is well known that the H α peak separation and the equivalent width correlate for the Be stars. Hanuschik et al. (1988) have derived the law

$$\log \left[\frac{\Delta V}{2v \sin i} \right] = -a \log \left[\frac{EW(\text{H}\alpha)}{\text{\AA}} \right] + b, \quad (1)$$

where ΔV is the peak separation, $v \sin i$ is the projected rotational velocity and $EW(\text{H}\alpha)$ is expressed in \AA . For stars with $EW(\text{H}\alpha) > 3 \text{ \AA}$, the average values are $a \simeq 0.4$ and $b \simeq -0.1$. In the limit case of the most dense envelopes $b = +0.2$. Since for rotationally dominated profiles $\Delta V/(2v \sin i)$ can be regarded as a measure of the outer radius inverse of the H α emitting disk (Hanuschik 1988), the law in Eq. 1 simply expresses that the outer radius grows as the $EW(\text{H}\alpha)$ becomes larger.

The same quantities for LS I+61°303 are plotted in Fig. 1 adopting $v \sin i = 360 \text{ km s}^{-1}$ (Hutchings & Cramp-ton 1981). The solid line represents the best linear fit over Rozhen data, from which we derive: $a = 0.38 \pm 0.04$ and $b = 0.07 \pm 0.04$. The dashed lines represent the average law ($a = 0.4$, $b = -0.1$) and the upper limit for the Be stars as obtained by Hanuschik et al. (1988). Using their formulation, our results imply that the circumstellar disk in LS I+61°303 is among the densest disks in the Be stars, i.e., roughly a factor of 2 denser than the average.

Dense circumstellar disks, optically thick at infrared wavelengths, have been recently identified in other Be/X-ray binaries (V0332+53, Negueruela et al. 1999; 4U 0115+63, Negueruela et al., in preparation). These works suggest that the disks around Be stars in X-ray binaries are denser and smaller than those in isolated Be stars. The results of Reig et al. (1997b) point towards neutron star preventing the formation of an ex-

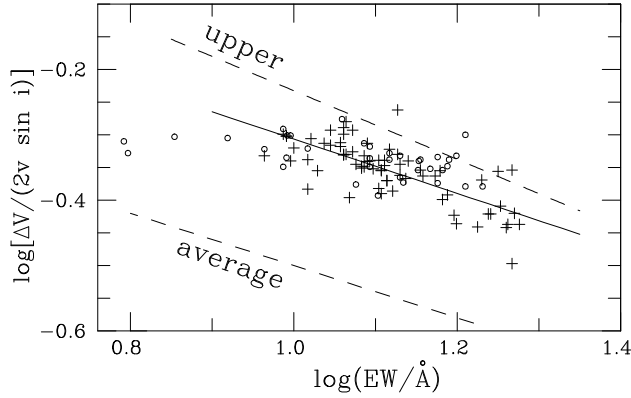


Fig. 1. Plot of $\log(\Delta V/(2v \sin i))$ versus $EW(H\alpha)$ of LS I+61°303. The crosses represent the Rozhen data, the circles the other. The solid line is the best linear fit over the Rozhen data. The dashed lines are the average behavior and the upper limit for the Be stars. It is visible that all data points are shifted towards denser Be disks

tended disk in systems with short orbital periods, presumably due to tidal truncation (Okazaki 1998).

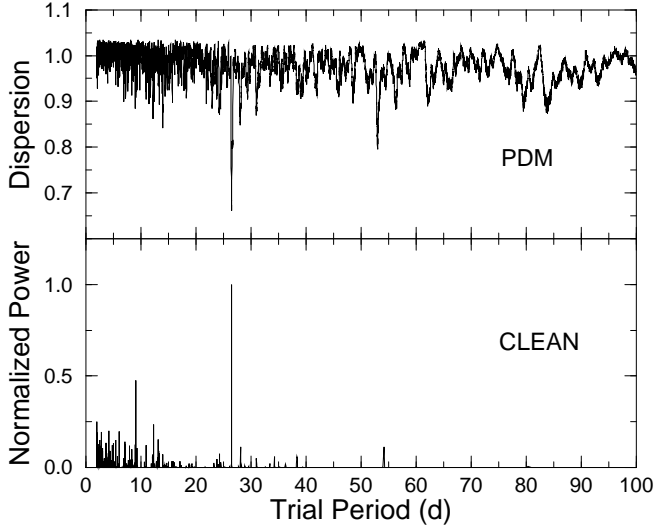


Fig. 2. Periodograms for the ratio $EW(B)/EW(R)$ in the $H\alpha$ emission line of LS I+61°303 computed using the PDM (top) and CLEAN (bottom) algorithms. The 26.5 d period is independently detected in both cases as the most significant one

3.2. Detection of 26.5 day period in $H\alpha$

We have conducted a period analysis for the different $H\alpha$ line parameters listed in Table 1. The period search methods used were both the Phase Dispersion Minimization (PDM) (Stellingwerf 1978) and the CLEAN algorithm (Roberts et al. 1987). As a result, we find clear evidences that the $H\alpha$ emission in LS I+61°303 also displays variations with the same 26.5 d radio period. This behavior is better revealed in the line ratios

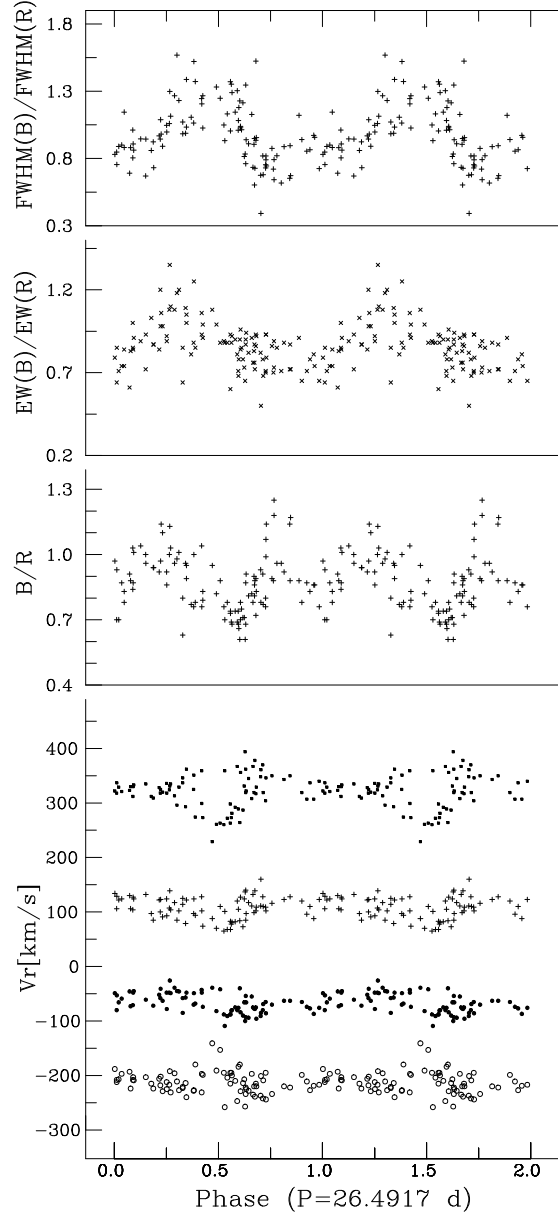


Fig. 3. $H\alpha$ line parameters of LS I+61°303 folded on the 26.4917 day period and zero phase set at JD2443366.775. The panel of radial velocities contains, from the lower to the upper plot, the heliocentric radial velocities of the blue hump, $V_r(B)$, the central dip, $V_r(dip)$, the red hump, $V_r(R)$, and the hump separation, ΔV , respectively

such as $FWHM(B)/FWHM(R)$, $EW(B)/EW(R)$ and B/R . The periods detected are about 26.50 – 26.55 d with typical error about ± 0.04 d. In Fig. 2 we present the PDM and CLEAN periodograms for the $EW(B)/EW(R)$ case. In this representative example, the most significant period detected in the range 2 – 100 d corresponds to 26.51 ± 0.03 d and 26.53 ± 0.04 d for the PDM and CLEAN methods, respectively. The first sub-harmonic at 53 d is also clearly noticeable in the PDM panel. The periodograms for the remaining line parameters, such as radial velocities and equivalent widths alone,

may also contain some power at the 26.5 d period. However, in most cases the detections are still too noisy and additional observations will be needed to confirm them.

In any case, Fig. 2 can be considered as a reliable proof that the signature of the LS I+61°303 radio period is present in the $H\alpha$ line.

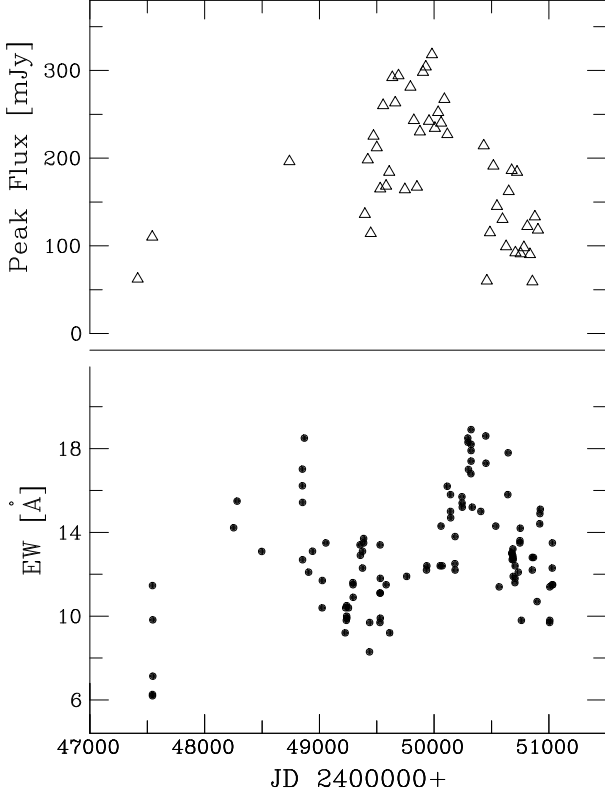


Fig. 4. Long term behavior of the $H\alpha$ equivalent width of LS I+61°303. The upper panel represents the radio outburst peak flux from Gregory (1999)

The $H\alpha$ parameters folded on the radio period, are displayed in Fig. 3 and illustrate the general trend of the $H\alpha$ orbital modulation. We used for this plot the 26.4917 d period value from radio wavelengths as the best estimate of the orbital cycle currently available (Gregory et al. 1999). In the panel of the radial velocities only the Rozhen and Crimean data are included. All data from Table 1 as well as the data from Paredes et al. (1994) are incorporated in other panels. The ratio $FWHM(B)/FWHM(R)$ achieves maximal values at radio phases 0.3 – 0.6. The equivalent width ratio has one well defined maximum at phases 0.25 – 0.4. In the B/R ratio at least one maximum is visible at phase 0.25, which coincides with the maximums of $FWHM(B)/FWHM(R)$ and $EW(B)/EW(R)$. A second maximum is visible at phase 0.8. It deserves noting that the appearance of this maximum is mainly due to 5 old points, which are very noisy and the presence of this maximum must be confirmed by future observations. These results proof the previous suggestions by Paredes

et al. (1994) and Zamanov et al. (1996) that an orbital variability in the line ratios exists.

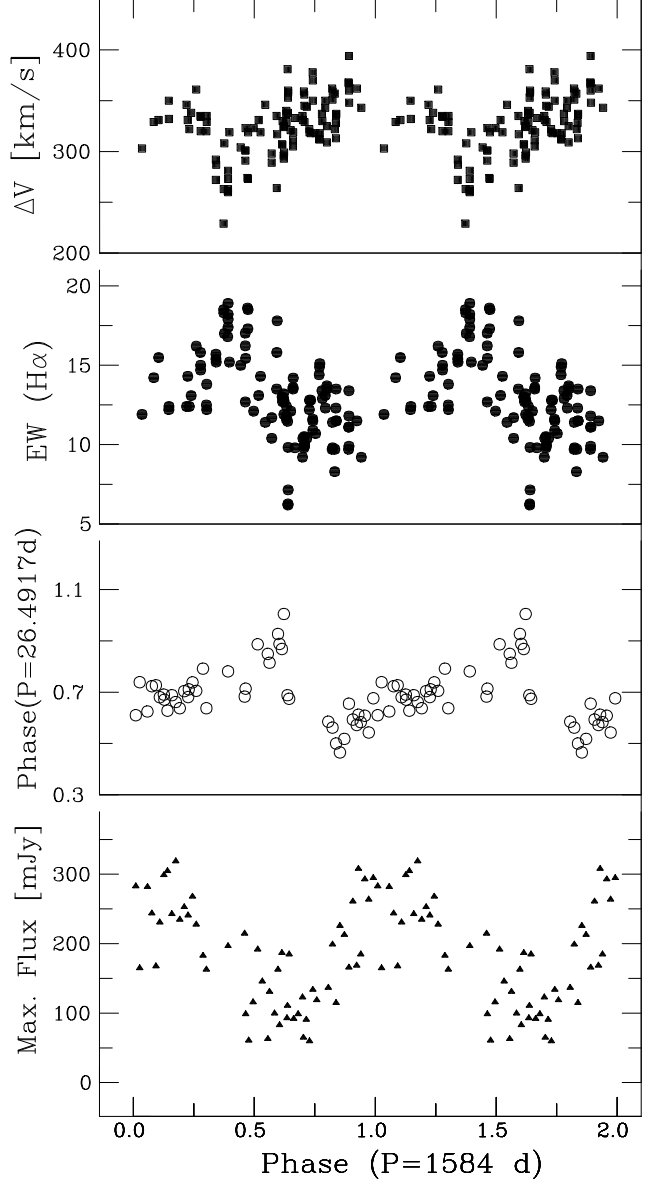


Fig. 5. $H\alpha$ and radio parameters of LS I+61°303 folded on the 1584 day period with zero phase set at JD2443366.775. From up to down are plotted the hump separation of the $H\alpha$, the total $EW(H\alpha)$, the phase of the radio maximum with respect to the 26.5 day period, and the maximum radio flux

3.3. Detection of a possible ~ 4 yr modulation in $H\alpha$

Fig. 4 represents the long term evolution of the $EW(H\alpha)$, which varies over the range 8–20 Å. These are real variations in the $H\alpha$ emitted flux, because the photometric observations of Mendelson & Mazeh (1995) have shown that the R -band flux is stable with maximal deviation of the points from the average

± 0.03 magnitudes only. Two maxima in the $EW(H\alpha)$ are visible, at about JD 2448850 and JD 2450300. The time interval between these two maxima is ~ 1500 d, which is remarkably close to the 1605 day period of the radio modulation as estimated by Martí (1993) and 1584 days by Gregory et al. (1999).

We have performed the period search for long term modulation. Although the values obtained are not well constrained they also point towards the four year modulation.

In Fig. 5 the H α line parameters $EW(H\alpha)$ and $\Delta V = V_r(R) - V_r(B)$ are plotted together with the radio parameters - the phase of the radio outburst and the maximum radio flux. The radio data are taken from Gregory (1999). All data are folded on the 1584 day period. Although the scatter of the points is considerable, the trend of this plot strongly suggests that the ~ 4 yr modulation in the H α line is very likely to be real.

3.4. Other period and correlation searches

In addition to the $EW(H\alpha)$, we also tried to find evidence for long term periodicities (100-2000 days) in other line parameters. The presence of B/R and related variability cycles, with periods between 4 months and 3 years, is currently regarded as a common characteristic of Be/X-ray binaries (Negueruela et al. 1998). Similar variability cycles exist in isolated Be stars, with longer periods ranging from 2 years to decades, with an average of 7 years. In those cases, the periodic variability is interpreted as due to the propagation of global density waves in the circumstellar disk (Okazaki 1997). Unfortunately, the results of this search turned out to be negative. Thus, the suggestion of a ~ 4 yr H α modulation remains present in the $EW(H\alpha)$ and the hump separation measurements.

Possible correlations between the $EW(H\alpha)$ and the radio outburst amplitude were investigated as well. We used for this purpose the NSF-NRAO-NASA Green Bank Interferometer data analyzed by Gregory (1999). For every H α data point, the closest radio maximum was selected and correlations were searched for. Again, none was found in reliable way. We do not rule out that all these negative results are a consequence of the considerable scatter of the points, not to say our still short time baseline for long term period studies. It deserves noting that the radio observations are missing just about the time of the $EW(H\alpha)$ maximum at JD2450300 and the H α observations are very sparse at the maximum of the radio flux modulation (see Fig. 4).

4. Discussion

4.1. The 26.5 day period and the Be envelope

Our spectroscopic results have provided a direct connection between the periodic radio outbursts of LS I+61°303 and its Be disk environment. This connection is based on the suggestive evidence that some of the H α emission line parameters also vary with the same 26.5 d and possibly ~ 4 yr periods previously found at radio wavelengths. Therefore, the outburst mod-

els based on the interaction between the compact object and the star Be envelope are clearly supported.

In this context, it appears likely that the 26.5 d H α variations have to be interpreted as the neutron star perturbing the Be envelope as it was discussed by Zamanov et al. (1996). However, other alternatives cannot be completely ruled out. For instance, the detected 26.5 d period in B/R and other ratios could also be caused by the propagation of a global density wave, as it happens in many Be X-ray binaries and isolated Be stars. This scenario would then imply the shortest propagation period of the global oscillation detected so far, and the first system in which the propagation of the density wave is synchronized with the orbital period of the neutron star.

4.2. What causes the ~ 4 yr modulation in LS I+61°303?

The H α observations presented here can be also used to discriminate between the two previously proposed models for the ~ 4 yr modulation in the radio outburst amplitude. In the LS I+61°303 case, it appears that the precessing jet model should be ruled out in favor of those based on quasi-cyclic Be-star envelope variations. Indeed, the most likely explanation of the $EW(H\alpha)$ changes, that we observe in a ~ 4 yr time scale, is a variability of the mass loss rate of the Be star.

To better assess this issue, it is instructive to obtain an estimation of how much the mass loss rate should change to account for the observed variations. We will use for this purpose the formulae of Vögel (1993) for an optically thin emission line. Of course, the H α line is probably not thin, so it must be considered as a rough estimation of the mass loss rate variability. The flux of a wind line determined by recombination can be represented as

$$F = \frac{h\nu}{4\pi d^2} \int_V \alpha_{\text{eff}}(n_e, T_e) n_e n_{\text{ion}} dV, \quad (2)$$

where d is the distance to the star, n_e is the electron density, n_{ion} the density of the ion considered, $\alpha_{\text{eff}}(n_e, T_e)$ is the effective recombination coefficient of the line, and V the emitting volume. In the circumstellar disk of LS I+61°303 the density follows the power law $\rho(r) = \rho_0(r/R_*)^{-3.25}$ (Waters et al. 1988), so the LS I+61°303 flux in H α can be expressed as

$$F = A \dot{M}_{\text{loss}}^2 \left[1 - \left(\frac{R_{\text{in}}}{R_{\text{out}}} \right)^{3.5} \right] \quad (3)$$

where \dot{M}_{loss} is the mass loss rate of the Be star, R_{in} and R_{out} are the inner and outer radius of the H α emitting disk, and the constant A includes the average recombination coefficient, the helium abundance and so on (for more details e.g. Vögel, 1993; Tomov et al. 1998). We adopt that $R_{\text{in}} = R_*$ and for Keplerian disk $\Delta V / (2v \sin i) = (R_{\text{out}}/R_*)^{-1/2}$ (Hanuschik 1988), where ΔV and $v \sin i$ are the same as in Section 3.1. Since $F \propto EW$, the observed H α parameters of LS I+61°303 correspond to

$$\dot{M}_{\text{loss,max}} / \dot{M}_{\text{loss,min}} \simeq 1.5. \quad (4)$$

In this way, the variability in $EW(H\alpha)$ can be explained by suggesting that the mass loss rate varies by a plausible amount of ± 25 per cent over its average value. This mechanism will also imply variations of the density over the same range.

The interaction of a neutron star with the Be star wind is critical in all suggested models for the radio outbursts of LS I+61°303. The variability of the mass loss rate of the Be star causes a variability of the mass accretion rate onto the neutron star in case of accretion onto the magnetosphere. In the model of young radio pulsar, the variability of the Be star mass loss changes the position of the shock front. In ejector-propeller model it affects the moments of switching of the Ejector - at lower mass loss rate we expect the ejector to switch on earlier and the radio outburst to peak at an earlier orbital phase than at higher mass loss rate.

In Fig. 5, it appears that the $H\alpha$ measurements are not in phase nor in anti phase with the radio data. This can be due to the bad distribution of the observations as it was noted above or to a real phase shift between the $H\alpha$ and radio parameters. At this moment we are only able to say that the 1600 day modulation detected in the phase variations of the 26.5 day periodic radio outbursts and the outburst peak flux density is visible in the $H\alpha$ emission line too.

In any case, it is clear that additional theoretical work and spectroscopic observations will be necessary to find out what is the exact relationship between the radio outbursts and the circumstellar disk.

4.3. Expectations at other wavelengths

Finally, if the ~ 4 yr modulation in radio and $H\alpha$ is due to changes in the circumstellar disk density, it can be probably detected as well in other wavelength domains. For instance, we can expect it to be visible in the infrared bands, where the circumstellar disk contributes with an excess above the stellar continuum. The X-rays and γ -rays may also be modulated every ~ 4 yr too, since the high energy emission of the neutron star depends on the density of the surrounding matter with which it interacts.

5. Conclusions

The main results from our $H\alpha$ spectroscopic observations of LS I+61°303 are:

1. The circumstellar disk in LS I+61°303 is among the densest of Be stars.
2. The 26.5 day period is visible in the $H\alpha$ emission line. This is the first time that a clear stable periodicity is detected in the $H\alpha$ emission line of a Be/X-ray binary in connection with the orbital motion of the compact object.
3. Evidences of a ~ 4 yr modulation in the $H\alpha$ of LS I+61°303 have been found. This favours the ~ 4 yr cycle in the radio outbursts as being related to variations of the circumstellar disk. The model of precessing jets should be consequently ruled out.

4. The ~ 4 yr modulation is also likely to be present at the infrared, X-ray and γ -ray domains.

Acknowledgements. RZ acknowledges support from the Bulgarian NSF (MUF-05/96). JMP and JM acknowledge partial support by DG-ICYT (PB97-0903). MR is supported by a fellowship from CIRIT (Generalitat de Catalunya, ref. 1999 FI 00199). JM is also partially supported by Junta de Andalucía (Spain).

References

- Bignami G.F., Caraveo P.A., Lamb R.C., Markert T.H., Paul J.A., 1981, *ApJ* 247, L85
- Coe M.J., Everall C., Fabregat J., et al., 1993, *A&AS* 97, 245
- Gregory P.C., Huang-Jian Xu, Bachhouse C.J., Reid A., 1989, *ApJ* 339, 1054
- Gregory P.C., Taylor A.R., 1978, *Nat* 272, 704
- Gregory P.C., Taylor A.R., Crampton D., et al., 1979, *AJ* 84, 1030
- Gregory P.C., 1999, *ApJ* 520, 361
- Gregory P.C., Peracaula M., Taylor A.R., 1999, *ApJ* 520, 376
- Hanuschik R.W., 1988, *A&A* 190, 187
- Hanuschik R.W., Kozok J.R., Kaiser D., 1988, *A&A* 189, 147
- Howarth I., Murray J., Mills D., et al., 1996, *Starlink User Note* 50, Rutherford Appleton Laboratory, U.K.
- Hutchings J.B., Crampton D., 1981, *PASP* 93, 486
- Ilyin I., 1997, *Licentiate Dissertation*, University of Oulu
- Kniffen D., Alberts W.C.K., Bertsch D.L., et al., 1997, *ApJ* 486, 126
- Maraschi L., Treves A., 1981, *MNRAS* 194, 1
- Martí J., 1993, *PhD Thesis*, University of Barcelona
- Mendelson H., Mazeh T., 1994, *MNRAS* 267, 1
- Negueruela I., Reig, P., Coe M.J., Fabregat J., 1998, *A&A* 336, 251
- Negueruela I., Roche P., Fabregat J., Coe M.J., 1999, *MNRAS* 307, 695
- Okazaki A., 1997, *A&A* 318, 548
- Okazaki A., 1998, in *IAU Coll 169 "Variable and non-spherical stellar winds in Luminous Hot Stars"* (in press)
- Paredes J.M., 1987, *PhD Thesis*, University of Barcelona
- Paredes J.M., Martí J., Estalella R., Sarate J., 1991, *A&A* 248, 124
- Paredes J.M., Martí J., Peracaula M., Ribó M., 1997, *A&A* 320, L25
- Paredes J.M., Marziani P., Martí J., et al., 1994, *A&A* 288, 519
- Reig P., Coe M.J., Stevens J.B., et al., 1997a, in *2nd INTEGRAL Workshop "The Transparent Universe"*, ESA SP-382, 175
- Reig P., Fabregat J., Coe M.J., 1997b, *A&A* 322, 193
- Roberts D.H., Lehar J., Dreher J.W., 1987, *AJ* 93, 968
- Shortridge K., Meyericks H., 1996, *Starlink User Note* 50, Rutherford Appleton Laboratory, U.K.
- Stellingwerf R.F., 1978, *ApJ* 224, 953
- Strickman M.S., Tavani M., Coe M.J., et al., 1998, *ApJ* 497, 419
- Tavani M., 1994, in *The Gamma-Ray Sky with GRO and SIGMA*, Dordrecht: Kluwer, 181
- Taylor A.R., Gregory P.C., 1984, *ApJ* 283, 273
- Taylor A.R., Kenny H.T., Spencer R.E., Tzioumis A., 1992, *ApJ* 395, 268
- Tomov N.A., Tomova M.T., Raikova D.V., 1998, *A&AS* 129, 479
- Vögel M., 1993, *A&A* 274, L21
- Waters L.B.F.M., Taylor A.R., van den Heuvel E.P.J., Habets G.M.H.J., Persi P., 1988, *A&A* 198, 200
- Zamanov R.K., 1995, *MNRAS* 272, 308
- Zamanov R., Paredes J.M., Martí J., Markova N., 1996, *Ap&SS* 243, 269

Table 1. H α line parameters of LS I+61° 303

Date (yyymmdd)	JD–2400000	$-EW(H\alpha)$ (Å)	$V_r(R)$ (km s $^{-1}$)	$V_r(B)$ (km s $^{-1}$)	$V_r(\text{dip})$ (km s $^{-1}$)	$EW(B)/EW(R)$	B/R	$FWHM(B)$ (Å)	$FWHM(R)$ (Å)
Ro920903	48869.50	18.5	110	-209	-69	0.68	0.77	4.55	6.68
Ro921009	48905.48	12.1	130	-193	-46	0.61	0.91	3.65	5.27
Ro930205	49024.27	10.4	83	-215	-88	0.60	0.73	5.55	5.52
Ro930206	49025.30	11.7	105	-184	-76	0.68	0.68	5.57	5.15
Ro930825	49225.45	9.2	132	-203	-61	0.93	0.96	5.43	5.75
Ro930829	49228.50	10.4	139	-192	-26	1.35	1.13	7.47	5.76
Ro930905	49235.49	9.8	101	-258	-109	0.88	0.70	5.85	6.27
Ro930907	49237.50	10.5	127	-229	-84	0.96	0.78	6.02	5.86
Ro930908	49238.53	10.0	117	-228	-94	0.82	0.81	5.61	6.17
Ro930909	49239.50	9.9	109	-220	-96	0.92	0.83	5.82	6.09
Ro931031	49292.30	11.6	139	-239	-78	0.72	0.88	3.42	4.68
Ro931101	49293.32	11.5	128	-242	-80	0.78	0.91	3.57	4.35
Ro931102	49294.49	10.9	116	-234	-70	0.86	0.89	3.61	4.12
Ro940101	49354.22	13.4	129	-208	-53	0.85	0.93	3.00	3.96
Ro940103	49356.28	12.9	127	-203	-48	0.84	0.87	3.40	3.74
Ro940122	49375.50	13.1	123	-220	-63	0.88	0.92	3.37	3.79
Ro940123	49376.27	12.3	128	-222	-63	0.87	0.88	3.13	3.49
Ro940201	49385.34	13.7	85	-224	-72	0.87	0.94	3.40	3.68
Ro940202	49386.27	13.5	123	-202	-41	0.98	0.97	3.65	3.36
Ro940624	49528.49	11.1	120	-247	-80	0.81	0.69	4.03	3.10
Ro940625	49529.49	13.4	137	-257	-100	0.65	0.61	3.59	4.30
Ro940626	49530.49	11.8	132	-235	-75	0.76	0.78	3.27	4.44
Ro940627	49531.47	11.1	111	-237	-91	0.82	0.93	3.08	4.54
Ro940818	49582.54	11.5	140	-222	-54	0.87	0.87	3.04	3.98
Ro960407	50181.30	12.5	91	-229	-63	0.98	1.10	3.17	3.55
Ro960408	50182.30	12.2	104	-231	-49	1.10	1.03	3.73	3.35
Ro960409	50183.36	13.8	102	-227	-46	1.20	1.01	4.35	3.54
Ro960608	50242.52	15.7	68	-204	-91	0.88	0.78	3.49	3.09
Ro960609	50243.52	15.4	82	-210	-75	0.90	0.74	3.29	2.88
Ro960610	50244.50	15.2	73	-214	-90	0.78	0.71	3.46	2.86
Ro960729	50293.55	18.5	88	-141	-39	1.08	0.95	—	—
Ro960730	50294.56	18.3	110	-153	-42	0.88	0.88	4.08	3.28
Ro960803	50298.59	17.0	111	-197	-55	0.91	0.82	3.57	3.17
Ro960824	50320.58	16.8	70	-191	-82	0.99	0.82	4.27	3.22
Ro960825	50321.53	18.2	65	-195	-88	0.89	0.76	3.89	3.71
Ro960826	50322.36	18.9	68	-195	-88	0.93	0.74	4.29	3.14
Ro960826	50322.49	17.4	78	-195	-81	0.88	0.69	4.19	3.11
Ro960827	50322.57	17.9	81	-200	-80	0.92	0.68	4.00	3.11
Ro970101	50450.36	18.6	94	-180	-68	0.85	0.78	4.65	3.40
Ro970102	50451.33	17.3	74	-199	-74	0.91	0.79	4.00	3.90
Ro970328	50536.26	14.3	85	-234	-93	0.90	0.68	4.13	3.08
Ro970426	50565.31	11.4	102	-244	-86	0.93	0.99	3.21	4.05
Ro970711	50641.47	15.8	84	-180	-40	0.90	0.61	3.93	3.21
Ro970713	50643.52	17.8	102	-215	-75	0.93	0.72	4.53	2.99
Ro970815	50676.50	13.0	96	-211	-74	0.71	0.87	3.10	3.62
Ro970816	50677.36	13.0	88	-219	-87	0.81	0.86	3.23	3.32
Ro970819	50680.56	12.7	106	-224	-73	0.83	0.88	2.85	3.23
Ro970824	50685.49	12.9	107	-217	-48	1.08	1.00	3.47	3.28
Ro970825	50686.47	13.2	85	-211	-45	1.18	0.98	4.49	2.88
Ro970826	50687.55	12.8	79	-214	-57	1.09	0.96	3.73	3.78
Ro970827	50688.59	11.9	97	-228	-70	0.88	0.76	3.71	3.49
Ro970828	50689.60	12.7	102	-197	-48	0.93	0.76	4.02	3.34
Ro970911	50703.38	11.6	110	-227	-77	0.78	0.83	3.07	3.54
Ro970912	50704.56	11.8	123	-217	-76	0.65	0.76	2.77	3.80
Ro970913	50705.54	12.4	122	-207	-66	0.71	0.70	3.04	3.41

Table 1. Continuation

Date (yyymmdd)	JD–2400000	$-EW(H\alpha)$ (Å)	$V_r(R)$ (km s ⁻¹)	$V_r(B)$ (km s ⁻¹)	$V_r(\text{dip})$ (km s ⁻¹)	$EW(B)/EW(R)$	B/R	$FWHM(B)$ (Å)	$FWHM(R)$ (Å)
Ro971010	50732.40	12.1	124	-197	-59	0.74	0.87	3.25	3.60
Ro980209	50854.21	12.2	97	-225	-66	0.94	0.91	3.12	3.32
Ro980210	50855.22	12.8	99	-220	-77	0.83	0.90	3.29	3.63
Ro980219	50864.23	12.8	106	-212	-80	0.64	0.70	3.14	3.70
Ro980323	50896.28	10.7	100	-218	-58	1.20	—	3.42	3.62
Ro980415	50919.27	14.4	104	-208	-71	0.85	0.84	2.89	3.58
Ro980417	50921.59	14.9	97	-215	—	1.03	—	3.17	3.68
Ro980419	50923.59	15.1	93	-225	-78	0.89	0.86	3.45	3.46
Ro980710	51005.56	9.7	122	-240	-48	1.05	0.89	4.88	3.53
Ro980711	51006.51	11.4	124	-227	-49	1.25	1.00	5.36	3.54
Ro980712	51007.49	9.8	128	-231	-43	1.06	1.04	4.41	3.55
Ro980802	51028.56	12.3	122	-206	-52	0.84	0.92	3.06	3.16
Ro980803	51029.53	11.5	124	-212	-48	0.92	0.92	3.37	3.22
Ro980804	51030.52	13.5	117	-196	-39	1.08	0.96	4.28	3.39
Ro980805	51031.56	11.5	114	-223	-58	0.85	0.80	3.68	3.44
SV921113	48939.80	13.1	111	-220	-62	0.81	0.77	3.62	3.29
SV930310	49056.70	13.5	93	-242	-95	0.85	0.96	3.30	3.98
SV930923	49253.90	10.4	96	-248	-65	1.06	1.14	3.94	4.01
SV940326	49437.34	8.3	90	-267	-101	0.72	1.00	2.72	3.96
SV940327	49438.37	9.7	66	-256	—	0.87	0.94	3.31	4.46
SV940624	49528.69	9.7	147	-221	-44	0.78	0.66	3.61	3.09
SV940626	49530.69	9.9	140	-220	-70	0.76	0.81	2.76	4.45
SV940916	49611.61	9.2	130	-213	-54	0.93	1.07	3.24	3.92
SV950212	49760.43	11.9	168	-135	23	1.00	0.95	3.81	3.69
SV950804	49933.73	12.2	126	-224	-53	0.91	0.88	3.12	2.81
SV950806	49935.70	12.4	128	-204	-62	0.74	0.86	2.98	3.10
SV960228	50141.43	15.8	132	-203	-56	0.70	0.80	2.87	3.86
SV960229	50142.39	15.0	131	-203	-55	0.70	0.88	2.88	3.92
SV960301	50143.40	14.7	122	-198	-53	0.71	0.96	2.67	4.20
SV971026	50747.52	13.6	91	-214	-73	0.84	0.70	3.12	3.01
SV971026	50747.66	13.5	103	-208	-73	0.85	0.75	3.19	3.15
SV971028	50749.48	14.2	113	-206	-54	0.86	0.89	3.08	3.28
Cr951129	50051.37	12.4	125	-221	-85	0.64	0.63	3.61	3.67
Cr951207	50059.21	14.3	124	-207	-66	0.73	0.71	3.00	3.68
Cr951217	50069.22	12.4	134	-188	-49	0.79	0.97	2.60	3.13
Cr960131	50114.32	16.2	160	-201	-85	0.50	0.78	2.51	6.40
Cr960904	50331.47	15.2	120	-199	-65	0.65	0.78	3.31	3.52
Cr961118	50406.33	15.0	109	-195	-65	0.71	0.76	2.75	3.65
Cr971107	50760.41	9.8	124	-209	-45	0.91	1.01	3.12	3.62

Ro: “Rozhen” Observatory; SV: Southampton & Valencia Universities collaboration; Cr: Crimean Astrophysical Observatory.